

Supplementary Table legends

Table S1

Xenopus and human proteins entries. Entries from all the *Xenopus laevis* proteins detected by mass spectrometry and the corresponding human protein entries.

Table S2

Ran Spindle Assembly Factors in the RanMT proteome. RanGTP regulated SAFs present in the RanMT proteome.

Table S3

The RanMT proteome. Complete human entries for the RanMT proteome after filtering and overlaps with previously published proteomes of interest. The following data are shown: spindle/MT related GOs; presence in MiCroKITS; or interaction with these; presence in the general RanMT network; number of connections in this network; presence in the functional networks; classification as a dynamic or non-dynamic protein and presence in any of the clusters. Ran SAFs, kinases and phosphatases are also specified.

Table S4

Protein candidates. Features of the selected protein candidates.

Table S5

Protein dynamic profiles. Clusters classification of the 286 dynamic proteins and their relative abundance values for each time-point.

Supplementary figure legends

Figure S1

Gene Ontology analysis of the RanMT proteome

Clusters of GO terms represented in the RanMT proteome obtained with the online CleverGO tool analysis. Three of the major clusters are shown in red with the corresponding Wordclouds on the left.

Figure S2

Candidate analysis

A- Western blot of control (CTRL) and CBX3 silenced cells using specific against anti-CBX3 and anti-tubulin antibodies. 30 μ g of cell protein lysate were loaded per lane. CBX3 was efficiently silenced.

B- Western blot of control (CTRL) and DnaJB6 silenced cells using specific against anti-DnaJB6 and anti-tubulin antibodies. 30 μ g of cell protein lysate were loaded per lane. DnaJB6 was efficiently silenced.

C- Schematic representation of the MT regrowth experiment in control and CBX3 or DnaJB6 silenced cells.

D- Schematic representation of the MT regrowth experiment in cells incubated with DMSO (control) or the CK2 inhibitor Quinalizarin.

Figure S3

Functional modules in the RanMT proteome

A- Venn diagram showing the overlap between the proteins (including the selected key factors and their interactors) present in each of the four functional modules. The table shows the number of proteins (selected key proteins and their interactors) in each module. Note that the total number of nodes and connections is smaller than the sum of all the individual categories due to overlaps.

B- Protein-protein interactome network of the proteins included in the MT nucleation module.

C- Protein-protein interactome network of the proteins included in the MT dynamics module including both MT stabilization and destabilization factors (green dots are proteins specific for MT-stabilization and blue dots are proteins specific for MT destabilization).

D- Protein-protein interactome network of the proteins included in the MT organization module.

In all cases only experimentally validated interactions were considered. The selected key proteins are in orange.

Figure S4

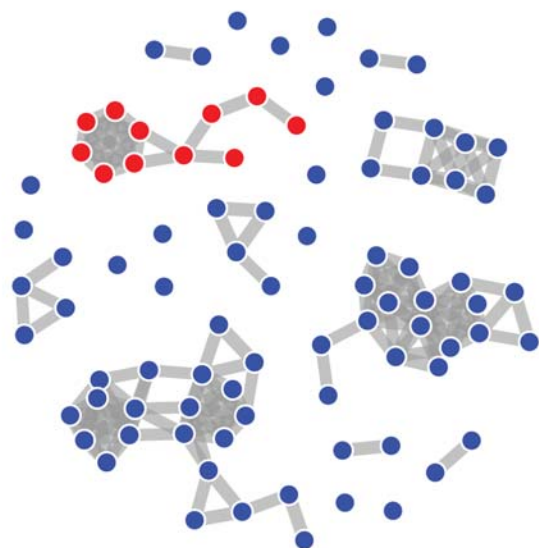
Intensity areas of the dynamic and non-dynamic proteins in the RanMT proteome

The average of the intensity areas for all the dynamic (white boxes) and non-dynamic (grey boxes) proteins in the RanMT proteome were calculated at each time point. Box and whiskers plot showing protein intensity area averages comparison between dynamic (white) and non-dynamic proteins (grey). Boxes show values between the 25th and the 75th percentiles, with a line at the median and a + at the mean, whiskers extend from the 10th to the 90th percentile and dots correspond to outliers values. No significant differences were observed between the two groups at any of the time-points (ANOVA test).

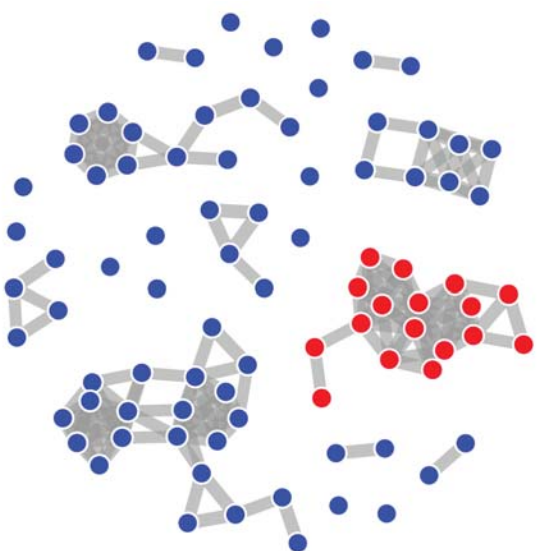
Figure S5

Dynamic abundance profiles for selected proteins and protein complexes

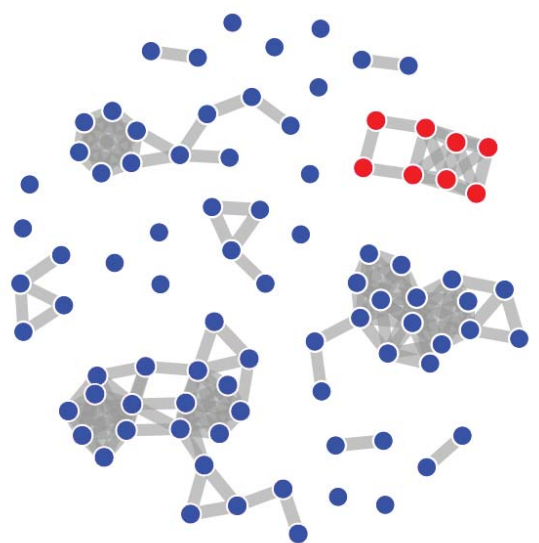
Graphical representation of the changes in relative protein abundance for some key proteins (as indicated) involved in (A) MT nucleation (cluster 6), (B) MT dynamics (clusters 5 and 6) and (C) MT organization (clusters 6 and 7).

A

mitochondrion
part Golgi lumen
microbody
apparatus
membrane **peroxisomal**
matrix peroxisome
reticulum endosome mitochondrial
endoplasmic

B

condensed MLL5L MLL12 MLL1
transcription centromeric methyltransferase cyclindependent
nuclear kinase THO
nucleolus periphery body
histone nucleoplasm
complex chromosome
matrix region acetyltransferase export protein part speck
activating holoenzyme

C

subunit small mitochondrial cytosolic
ribosomal
large organellar

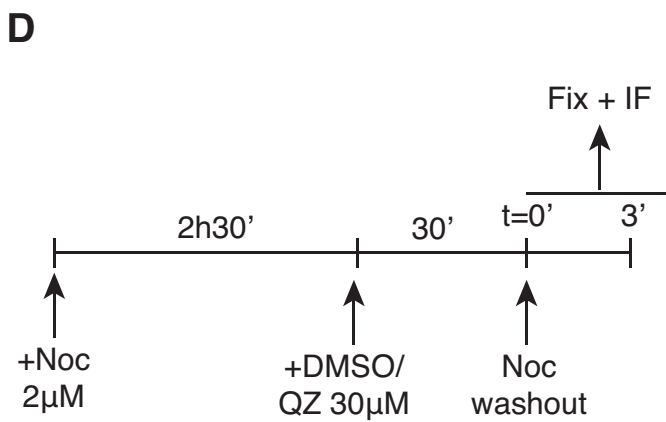
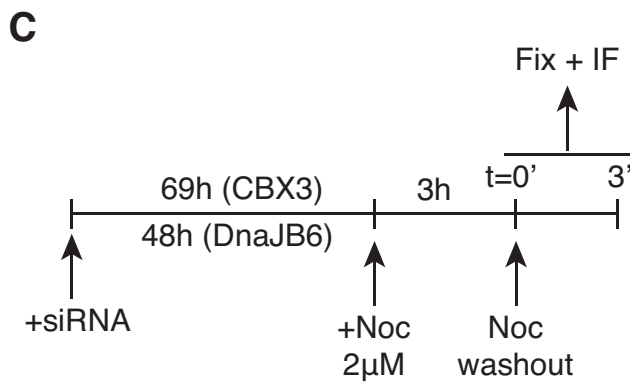
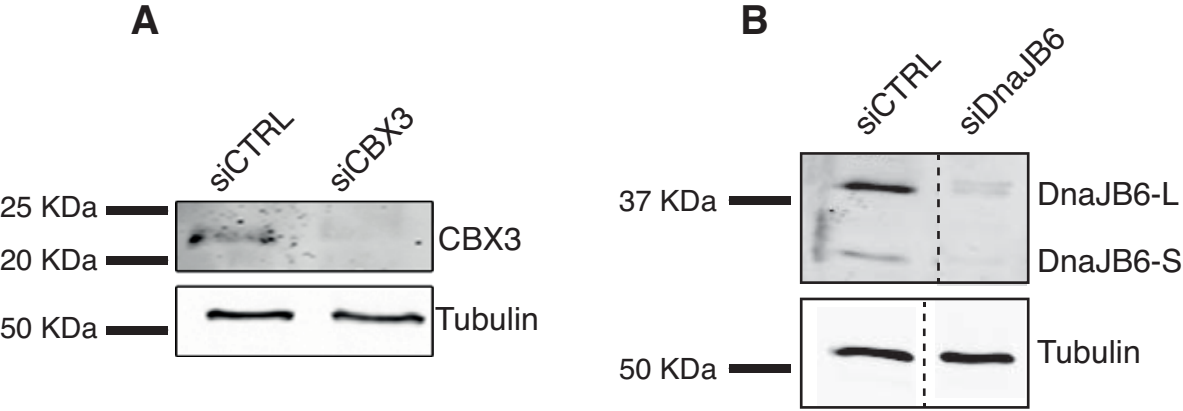
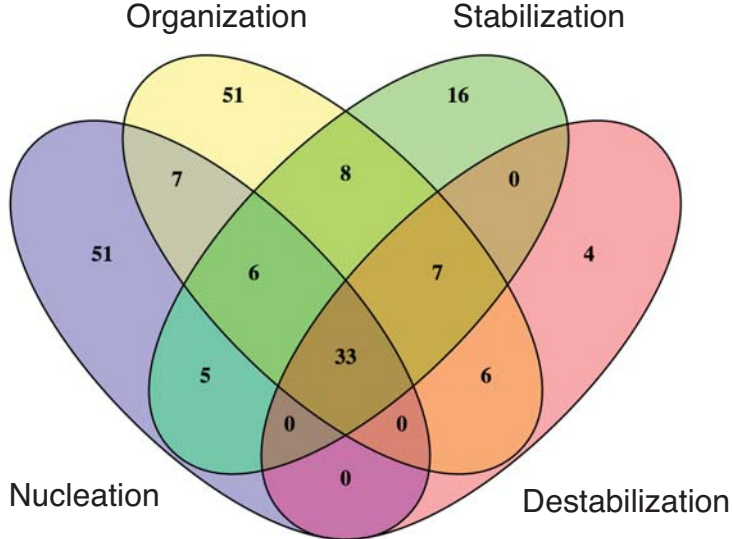


Figure S2

A



	Nodes	Connections
Nucleation	15	85
Stabilization	7	67
Destabilization	5	44
Organization	22	95
Total	47	142

B

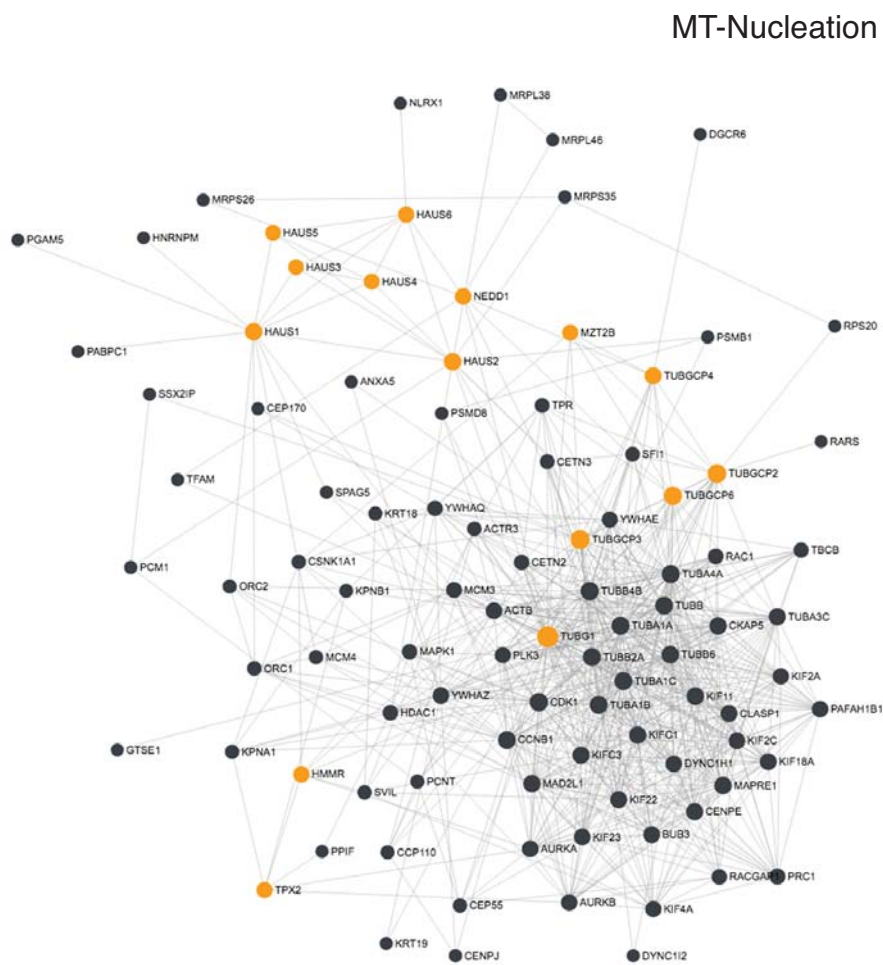
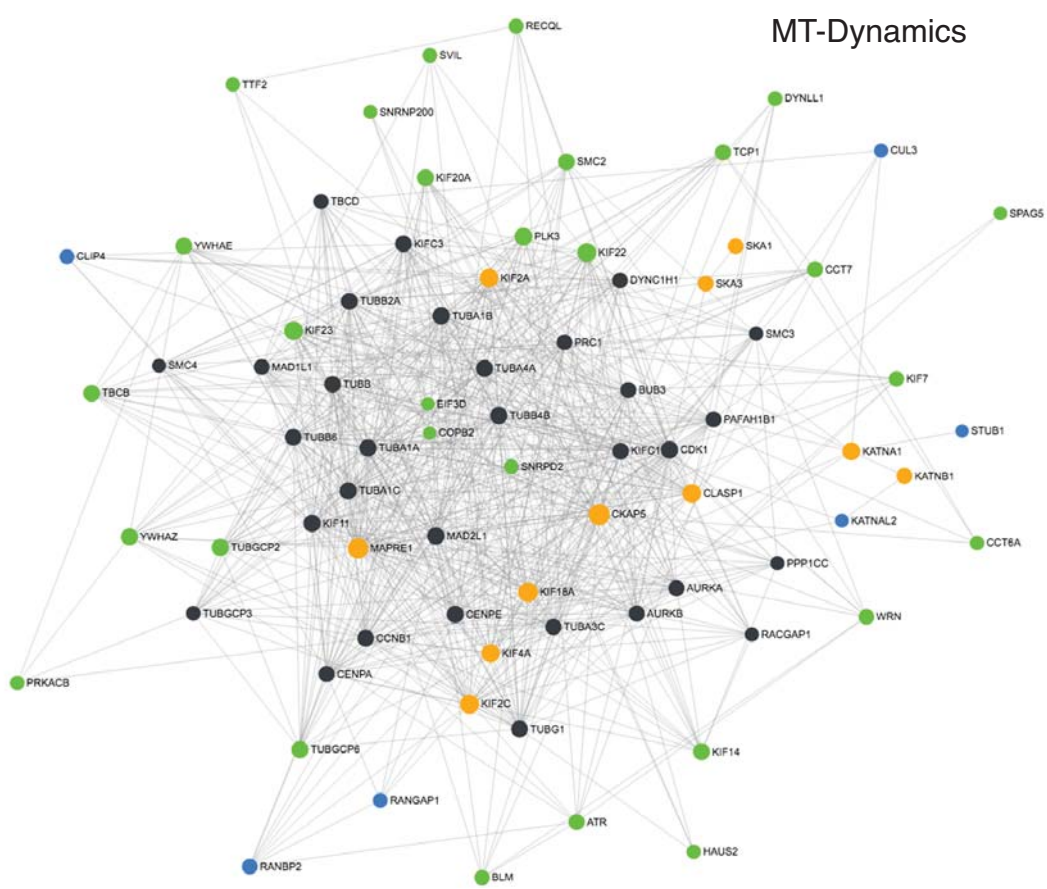
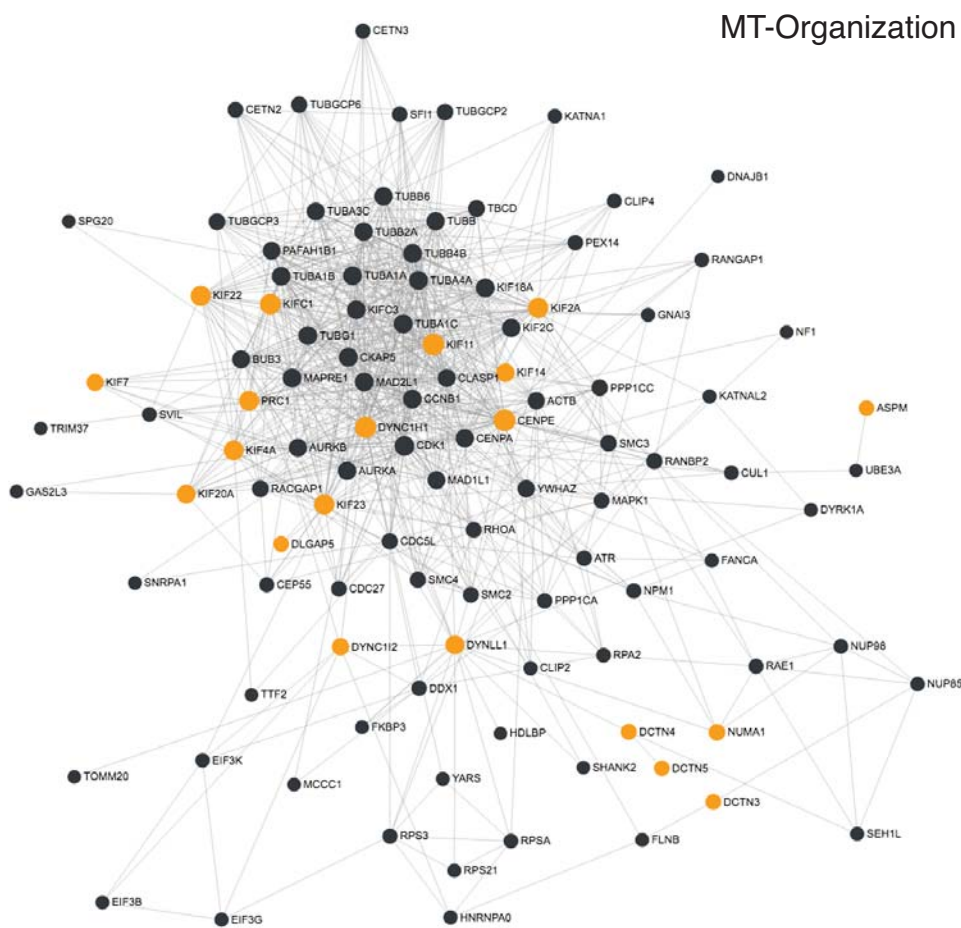


Figure S3

C**D****Figure S3**

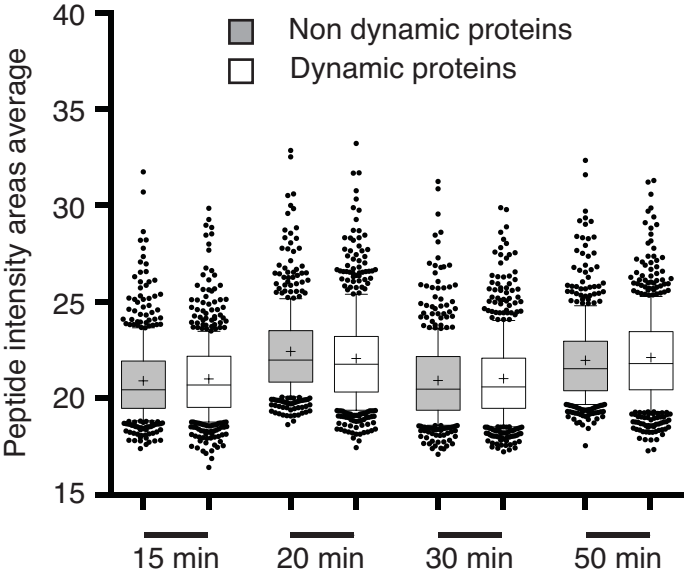
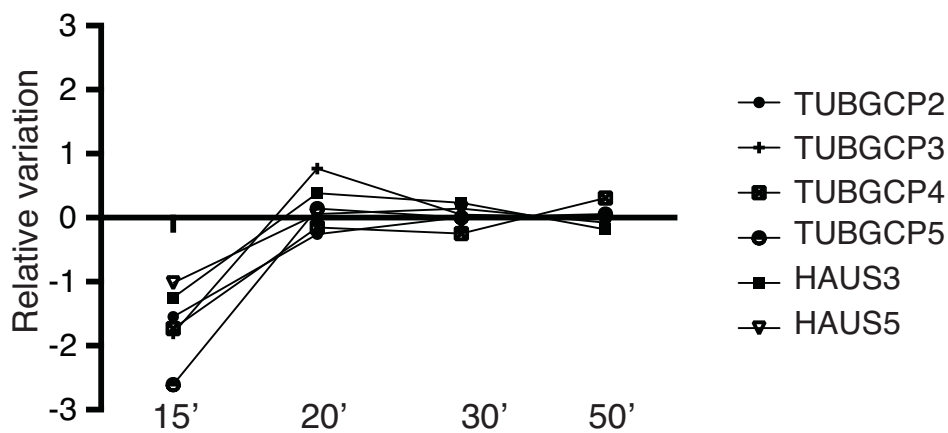
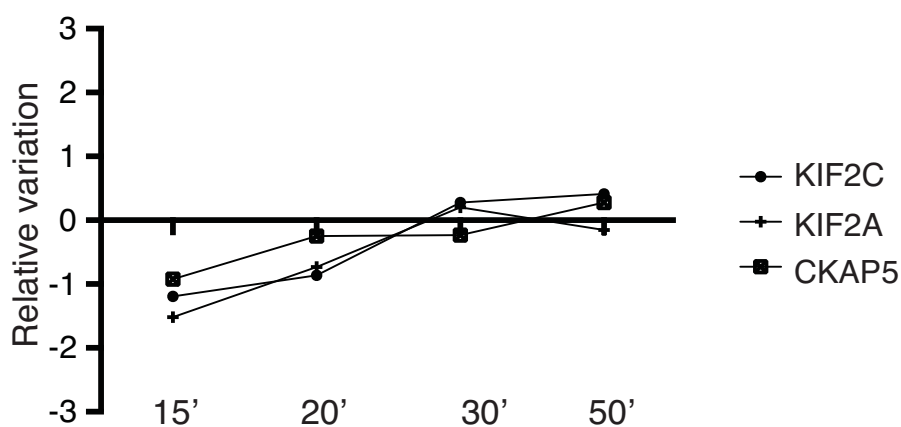
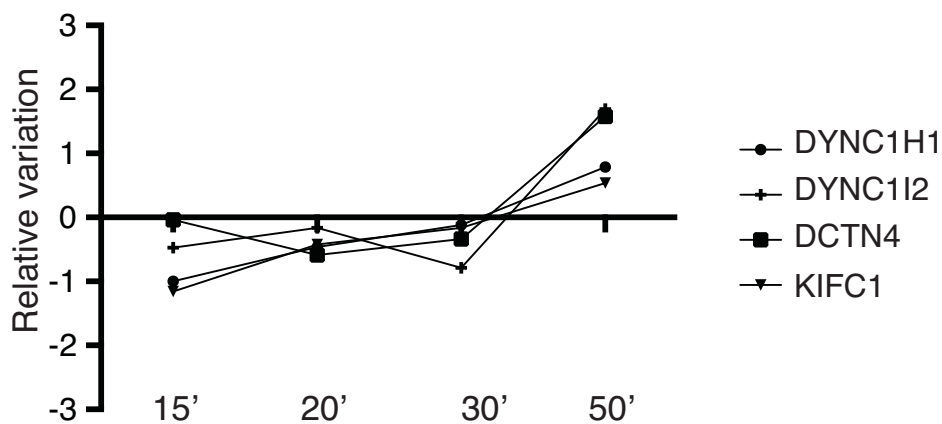


Figure S4

A**B****C****Figure S5**